RSC Advances

ROYAL SOCIETY OF CHEMISTRY

PAPER

View Article Online
View Journal | View Issue

Check for updates

Cite this: *RSC Adv.*, 2020, **10**, 7691

Open Access Article. Published on 21 February 2020. Downloaded on 12/9/2025 2:17:52 PM.
This article is licensed under a Creative Commons Attribution-NonCommercial 3.0 Unported Licence.

One-pot synthesis at room temperature of epoxides and linalool derivative pyrans in monolacunary $Na_7PW_{11}O_{39}$-catalyzed oxidation reactions by hydrogen peroxide†

Castelo B. Vilanculo, [*a] Márcio J. Da Silva, [b] Milena Galdino Teixeira [b] and Jesus Avendano Villarreal[c]

Received 2nd January 2020
Accepted 25th January 2020

DOI: 10.1039/d0ra00047g

rsc.li/rsc-advances

In this work, we describe a new one-pot synthesis route of valuable linalool oxidation derivatives (*i.e.*, 2-(5-methyl-5-vinyltetrahydrofuran-2-yl propan-2-ol) (**1a**)), 2,2,6-trimethyl-6-vinyltetrahydro-2*H*-pyran-3-ol (**1b**) and diepoxide (**1c**), using a green oxidant (*i.e.*, hydrogen peroxide) under mild conditions (*i.e.*, room temperature). Lacunar Keggin heteropolyacid salts were the catalysts investigated in this reaction. Among them, $Na_7PW_{11}O_{39}$ was the most active and selective toward oxidation products. All the catalysts were characterized by FT-IR, TG/DSC, BET, XRD analyses and potentiometric titration. The main reaction parameters were assessed. Special attention was dedicated to correlating the composition and properties of the catalysts and their activity.

1. Introduction

The oxidation of terpenic alcohols, which are an abundant, renewable and attractive raw material, provide compounds useful for the synthesis of fine chemicals, fragrances, perfumes, and agrochemicals.[1,2] Linalool is a tertiary alcohol whose cyclization derivatives and epoxides are highly valuable due to their chiral building blocks for the synthesis of drugs.[3,4] The cyclization of linalool is an intramolecular process that results in the formation of tetrahydropyran and tetrahydrofuran derivatives, which are compounds with potential biological activity.[5–7]

Several strategies have been developed to cyclize the linalool. Commonly, the first step of linalool cyclization requires a preliminary activation of the double bond through its transformation in epoxide or halogenate derivatives, which cyclizes to give the corresponding ether derivatives containing an additional hydroxyl or halogen functional group.[8,9] Nonetheless, these multistep processes have low atomic efficiency and involve the use of environmentally hazardous stoichiometric oxidants, resulting in residual wastes.[10]

In this regard, to develop oxidative routes of linalool based on hydrogen peroxide, an inexpensive, atom-efficient and green oxidant that generates only water as a by-product is a challenge to overcome.[11,12] Nonetheless, hydrogen peroxide requires the presence of a metal catalyst to be activated.[13]

Among the various catalysts used in oxidations with hydrogen peroxide, polyoxometalates should be highlighted due to their high compound versatility that has been effective in homogeneous and heterogeneous processes.[14–16] Several heteropolyacids have redox properties that characterize them as an efficient catalyst in oxidation reactions with oxygen or hydrogen peroxide.[17]

Keggin heteropolyacids (HPAs) are the most used polyoxometalates in catalysis. However, they are strong Brønsted acids, a feature that compromises their use as a catalyst in oxidations of monoterpenes, which are substrates susceptible to acid-catalyzed concurrent reactions such as carbon skeletal rearrangement and nucleophilic addition.[18,19] To circumvent this drawback, a rarely explored approach is to convert Keggin HPAs to neutral salts, exchanging their acidic protons by metal cations.[20,21] Moreover, the removal of one MO unit of heteropolyanions (*i.e.*, WO or MoO) results in a lacunar salt catalyst that may be more active than its precursor with saturated anion.[22–24]

The synthesis of linalool oxides and diepoxides, using lacunar polyoxometalates as catalysts, has not yet been reported in the literature. In this work, we present an innovative method of one-pot synthesis of linalool oxides with high conversion and selectivity, using a lacunar polyoxometalate as catalyst and hydrogen peroxide as an oxidant.

[a]Chemistry Department, Pedagogic University of Mozambique, FCNM, Campus of Lhanguene, Av. de Moçambique, Km 1, Maputo, 4040, Mozambique. E-mail: castelovilanculo@gmail.com; Tel: +258 825573337

[b]Chemistry Department, Federal University of Viçosa, Minas Gerais State, 36590-000, Brazil

[c]Chemistry Department Federal University of Minas Gerais, Minas Gerais State, 31270-901, Brazil

† Electronic supplementary information (ESI) available. See DOI: 10.1039/d0ra00047g

Open Access Article. Published on 21 February 2020. Downloaded on 12/9/2025 2:17:52 PM. This article is licensed under a Creative Commons Attribution-NonCommercial 3.0 Unported Licence.

We synthesized three lacunar Keggin HPAs sodium salts and assessed their catalytic activity on the oxidation of linalool by hydrogen peroxide. All the lacunar salts were characterized by FT-IR, BET, XRD, TG/DSC techniques and their acidity strength were measured by *n*-butylamine titration. The effects of the main reaction variables were analyzed.

2. Experimental section

2.1. Chemicals

Linalool was purchased acquired by Sigma-Aldrich (99 wt%). Sodium hydrogen carbonate from Vetec (99 wt%). All the HPAs (*i.e.*, $H_3PW_{12}O_{40}$, $H_3PMo_{12}O_{40}$, and $H_4SiW_{12}O_{40}$; 99 wt%) were purchased from Sigma-Aldrich. $Na_2WO_4\cdot 2H_2O$ from Vetec (99 wt%), $HCl_{(aq)}$ (33 wt%) from Dinâmica and aqueous $H_3PO_{4(aq)}$ (85 wt%) was from Sigma-Aldrich. CH_3CN was acquired from Sigma (99 wt%) Aqueous hydrogen peroxide was from Alphatec (35 wt%). All reagents were used as received without further purification.

2.2. Synthesis of lacunar Keggin heteropolyacid salts ($Na_7PW_{11}O_{39}$)

The lacunar sodium salts preparation is very similar and they were prepared according to the reported procedure[25]. The only difference is the pH range used. Only the synthesis of lacunar phosphotungstate sodium salt was highlighted. Typically, 1 g of hydrate $H_3PW_{12}O_{40}$ was dissolved in water (30 mL) and heated to 333 K with constant magnetic stirring. The solution's pH was adjusted to 4.8 using a $NaHCO_3$ solution (Scheme SM1†). This results in the formation of the lacunar anion $[PW_{11}O_{39}]^{7-}$. The solution with pH 4.8 was 3 h heated at 333 K. Finally, the $Na_7PW_{11}O_{39}$ salt was obtained by solvent evaporation and recrystallization from water, followed by drying 5 h at 373 K. Once the synthesis of other lacunar salts (*i.e.*, $Na_7PMo_{11}O_{39}$, $Na_8SiW_{11}O_{39}$) being very similar, it was omitted by simplification.

2.3. Synthesis of saturated sodium phosphotungstate salt ($Na_3PW_{12}O_{40}$)

For comparison, the sodium phosphotungstate catalyst was also synthesized.[20] $Na_2WO_4\cdot 2H_2O$ (30 mmol, 10 g) was slowly added to 20 mL of distilled water and the mixture was magnetically stirred and warmed to 333 K. Then, after to add $H_3PO_{4(aq)}$ (15 mmol, 1 mL) and $HCl_{(aq)}$ (100 mmol, 8 mL) the resulting mixture was stirred for 1 h. The white solid was washed with water and was recrystallized twice from hot water.

2.4. Characterization of catalyst

Infrared spectra (FT-IR) were obtained on Varian 660-IR spectrometer at wavenumber range from 500 to 1700 cm^{-1}, the fingerprint region of the main absorption bands of Keggin heteropolyanions. The bulk structure of the catalysts was examined by X-ray diffraction (XRD) technique on a Bruker D8-Discover diffractometer using Ni filtered Cu-kα radiation (λ = 1.5418 Å), working at 40 kV and 40 mA. The measurements were obtained with a count time of 1.0 s and in the 2θ range of 5–80 degrees.

Thermogravimetric analysis (TGA) was performed using a PerkinElmer Simultaneous Thermal Analyzer (STA) 6000, to study the thermal decomposition and verify the hydration degree of the fresh catalyst. The masses of the samples used were between 10–50 mg, with a heating rate of 10 °C min^{-1} under nitrogen flow. Thermogram temperatures were recorded at each 0.1 °C range over a range of 30–600 °C.

The surface area and total pore volume of the catalysts were measured by N2 physisorption/desorption technique using NOVA 1200e High Speed, Automated Surface Area, and Pore Size Analyzer Quantachrome Instruments. The samples were outgassed by 1 h. The surface area was calculated by the Brunauer–Emmett–Teller equation applied to the isotherms.

Catalyst acidity was estimated by potentiometric titration, as described by Pizzio *et al.*[26] The electrode potential variation was measured with a potentiometer (*i.e.* Bel, model W3B). Typically, 50 mg of HPA salt was dissolved in a CH_3CN solution, magnetically stirred for 3 h and then titrated with a *n*-butylamine solution in toluene (*ca.* 0.05 mol L^{-1}).

2.5. Identification of main reaction products

The major products were previously identified in a Shimadzu GC-2010 gas chromatographer coupled with a MS-QP 2010 mass spectrometer (*i.e.*, electronic impact 70 eV, scanning range of *m*/*z* 50–450). Afterward, they were purified by column chromatography (silica 60G) using eluent hexane, containing 20% of ethyl acetate. Products (**1a**, **1b**) were then characterized by ^1H and ^{13}C NMR and FT-IR (Varian FT-IR 660) spectroscopy analysis (see ESI†). The NMRs spectra were taken in $CDCl_3$ solutions, using a Varian 600 spectrometer at 600 and 150 MHz, respectively. The chemical shifts were expressed as δ (ppm) relative to the tetramethylsilane (TMS) as an internal reference. Due to low yield, it was not possible to characterize diepoxide **1c**; only their GC-MS data were obtained (see ESI†).

2.6. Catalytic runs

The catalytic tests were carried out in acetonitrile under air (atmospheric pressure) in a closed three-necked glass flask (25 mL), equipped with a sampling system and a reflux condenser, and immersed in a thermostatic water bath. Typically, linalool (2.75 mmol) was solved in a CH_3CN solution (*ca.* 10 mL), magnetically stirred and the reactions were carried out at room temperature. After the addition of the catalyst (*ca.* 0.33 mol%), the reaction was started and monitored during 4 h, periodically collecting aliquots and analyzing them in a GC equipment (Shimadzu 2010, FID).

3. Results and discussion

3.1. Catalysts characterization

The FT-IR study provides information about the Keggin anion structure (*i.e.*, primary structure); for instance, if it was retained or not after the removal of one WO unit. Fig. 1 shows infrared

Open Access Article. Published on 21 February 2020. Downloaded on 12/9/2025 2:17:52 PM.
This article is licensed under a Creative Commons Attribution-NonCommercial 3.0 Unported Licence.

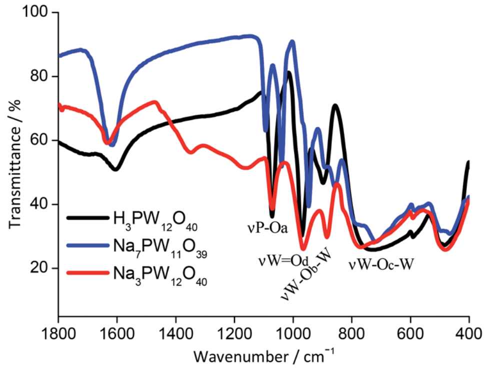

Fig. 1 FT-IR spectra of phosphotungstic acid, saturated sodium salt and lacunar sodium salt.

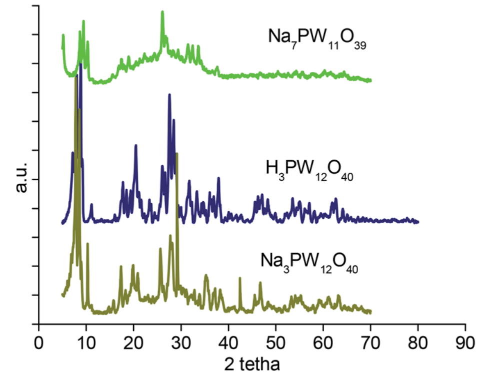

Fig. 2 Powdered XRD patterns of $Na_7PW_{11}O_{39}$ lacunar salt, parent $H_3PW_{12}O_{40}$ and saturated $Na_3PW_{12}O_{40}$.

spectra of Keggin phosphotungstate salts (*i.e.*, $Na_7PW_{11}O_{39}$ and $Na_3PW_{12}O_{40}$, respectively) and their parent heteropolyacid.

The main absorption bands of $H_3PW_{12}O_{40}$ were noticed at wavenumbers 1080, 980, 920, and 790 cm^{-1}, which agree with data of literature.[27] These bands were assigned to the stretching of P–O_a, W–O_d, W–O_b–W and W–O_c–W bonds. The main absorption bands of $Na_3PW_{12}O_{40}$ salt were like the pattern, meaning that the salt was successfully synthesized. The subscripts distinguish oxygen atoms; O_b are oxygen atoms belonging to the WO_6 octahedral units sharing corners, O_c referrers to the oxygen atoms in edges, and O_d are terminal oxygen atoms. All of them are connected to the tungsten atoms, while O_a are bonded to the phosphorous atom.[28]

The splitting of P–O_a bond absorption band at wavenumber 1080 cm^{-1}, which resulted in two new bands (*ca.* 1020 and 1060 cm^{-1}) is the main guarantee that the lacunar heteropolyanion was formed.[29–31] This splitting is assigned to the decreasing symmetry of PO_4 group, resultant from the removal of the WO unit.[32] The same effect occurred when the $Na_7PMo_{11}O_{39}$ lacunar salt was synthesized, nonetheless, the absorption bands appeared at wavenumbers 1078 and 1035 cm^{-1} (Fig. SM1†).[33] Conversely, when the $Na_8SiW_{11}O_{39}$ lacunar salt was synthesized, the stretching band of Si-O_a bond remained untouchable (Fig. SM2†).

While infrared spectra gave information about the primary structure of Keggin HPAs, XRD spectra provides data of the secondary structure. Fig. 2 shows clearly that the XRD spectrum of $Na_7PW_{11}O_{39}$ lacunar salt displayed different peak patterns than those presented by parent $H_3PW_{12}O_{40}$ and its saturated salt. It showed a lower level of crystallinity, with less intense peaks than the precursor heteropolyacid and the saturated phosphotungstate salt. This different crystallinity may be assigned to the exchange of protons by sodium cations and a changing on water hydration water molecules number (see Fig. 3). The other two lacunar sodium salts also presented a lower crystallinity level than acid precursors too (Fig. SM3 and SM4†).

TG/DTG curves obtained from lacunar $Na_7PW_{11}O_{39}$ showed two regions of weight loss; the first one before 473 K assigned to loss of all water molecules. The second one, was assigned to the decomposition of P–O_a–W framework followed by the noticeable peak in DSC curves around 793 K. The final products are an oxides mixture (Fig. 3).

TG curves of the lacunar salt presented a weight loss of around 10%, likewise the precursor acid (Fig. 3a and b); nevertheless, it has occurred more quickly for the heteropolyacid sample, indicating that the lacunar salt was thermally more stable. The same behaviour was also observed on TG curves of silicotungstic and phosphomolybdic acids and their respective lacunar sodium salts (Fig. SM5 and SM6†).

The titration curves of the lacunar sodium salts and their precursor Keggin HPAs were obtained (Fig. 4). This procedure allows to classify the acidity strength of acid sites; $E_i > 100$ mV (very strong sites), $0 < E_i < 100$ mV (strong sites), $-100 < E_i < 0$ (weak sites) and $E_i < -100$ mV (very weak sites).[34]

Regardless of the Keggin anion, the titration curves presented similar pattern; a quick decrease in the electrode potential after the addition of base minimum volume suggests that only a residual Brønsted acidity remained after the exchange of protons by the sodium cations, indicating that the protons were virtually removed.

After the initial period of the titration, the potential remained practically constant. This behaviour was completely distinct than the precursor heteropolyacids (Fig. 4, SM7 and SM8†).

The precursor HPA presented very strong acid sites (*i.e.*, E_i = 700 mV, inset in Fig. 4); the exchange of protons by the sodium cations reduced this acidity (E_i = 375 mV), however, it was

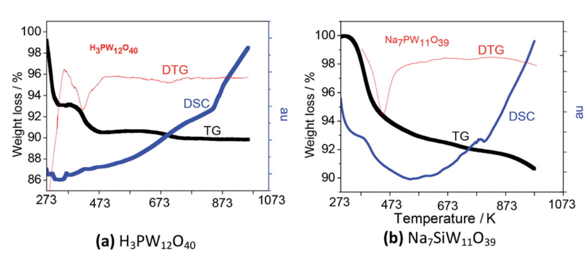

Fig. 3 TG/TDTG and DSC curves: precursor $H_3PW_{12}O_{40}$ (a) and lacunar salt $Na_7PW_{11}O_{39}$ (b).

Open Access Article. Published on 21 February 2020. Downloaded on 12/9/2025 2:17:52 PM. This article is licensed under a Creative Commons Attribution-NonCommercial 3.0 Unported Licence.

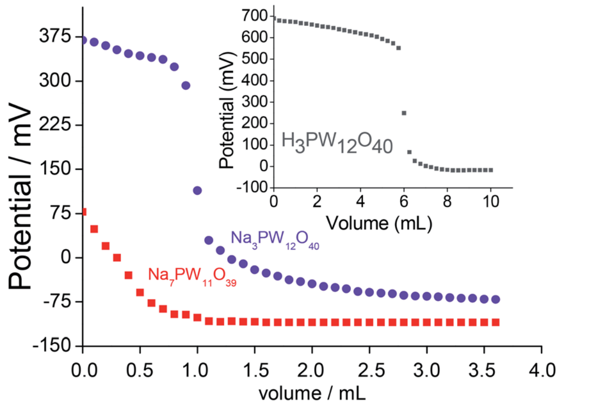

Fig. 4 Potentiometric titration curves with *n*-butylamine of $H_3PW_{12}O_{40}$, $Na_3PW_{12}O_{40}$ and $Na_7PW_{11}O_{39}$ catalysts.

classified as very strong. Conversely, lacunar salt was less acid (E_i = 75 mV). Their strong acid sites may be assigned to the residual protons (Fig. 4).

The pore sizes presented by sodium salts were very similar to those displayed by the parent acids (*ca.* 1–4 $m^2\ g^{-1}$), regardless of the Keggin anion. Aiming simplifies, only the isotherms and pores size distribution of the $Na_7PW_{11}O_{39}$ salt was shown in Fig. 5. The quick initial increase corresponds to the formation of the first layer; therefore, an increase in pressure forms the second layer of adsorbed molecules, followed by another layer. The total reversibility of the adsorption–desorption isotherm was observed (*i.e.*, absence of hysteresis cycle) for all catalysts, a condition noticed in this catalyst.

3.2. Catalytic tests

3.2.1. Effect of catalyst nature in linalool oxidation reactions with hydrogen peroxide. Initially, we have assessed the catalytic activity of the sodium phosphotungstate salts on the linalool oxidation with H_2O_2 (Fig. 6). The reaction conditions were chosen according to the literature.[1] The $Na_7PW_{11}O_{39}$ catalyst was more active than the lacunar ($Na_7PW_{11}O_{39}$ and mainly $Na_8SiW_{11}O_{39}$) or saturated salts ($Na_3PW_{12}O_{40}$) (Fig. 6a). This effect demonstrates the importance of the presence of the tungsten atoms as well as a vacancy on the heteropolyanion catalyst structure.

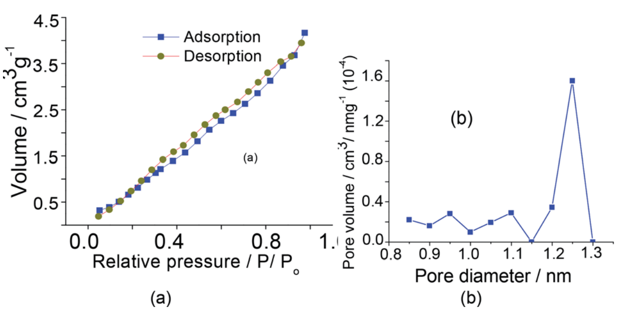

Fig. 5 Isotherms of adsorption and desorption (a), volume and diameters porous (b) of the $Na_7PW_{11}O_{39}$ catalyst.

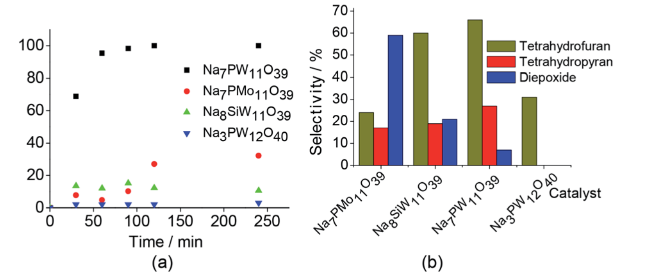

Fig. 6 Effect of catalyst nature on the conversion (a) and selectivity (b) of the linalool oxidation reaction with H_2O_2. [a]Reaction conditions: linalool to H_2O_2 (1 : 2); lacunar salt catalyst (0.33 mol%); temperature (298 K); CH_3CN (10 mL).

Although not included in the Fig. 6, the $H_3PW_{11}O_{39}$ -catalyzed oxidation reaction of linalool achieved only a poor conversion (*ca.* 9%) and no oxidation product was detected.

In addition to highest activity (conversion of *ca.* 100%), the lacunar $Na_7PW_{11}O_{39}$ catalyst was also the most selective toward the goal-products; *cis* and *trans* 2-(5-methyl-5-vinyltetrahydrofuran-2-yl propan-2-ol) (**1a**), *cis* and *trans* 2,2,6-trimethyl-6-vinyltetrahydro-2*H*-pyran-3-ol (**1b**), which were formed at equimolar proportions. The diepoxide (**1c**) was also obtained in linalool (**1**) oxidation reaction (Scheme 1).[6]

Note that the 2-(5-methyl-5-vinyltetrahydrofuran-2-yl propan-2-ol) (**1a**) and 2,2,6-trimethyl-6-vinyltetrahydro-2*H*-pyran-3-ol (**1b**) oxides were the major products, with selectivity of 66 and 27%, respectively (Scheme SM2†). On the other hand, the diepoxide (1c) had only a selectivity of 7% (Fig. 6b). It indicates that this catalyst system is highly selective for the synthesis of the linalool oxides. The formation of the tetrahydrofuran derivative (**1a**) with a five-members ring was more selective in all the reactions, excepted when the catalyst was $Na_7PMo_{11}O_{39}$. Probably, (**1a**) is the kinetic product and thus is formed faster than (**1b**) product, which has a six-member ring.

Conversely, the diepoxide (**1c**) was the major product in $Na_7PMo_{11}O_{39}$-catalyzed reaction and the secondary one in reaction with $Na_8SiW_{11}O_{39}$. As we will demonstrate, the epoxide is directly involved in the formation of linalool oxides.

3.2.2. Effect of the oxidant load on the oxidation of linalool. We suppose that an oxidant may play a crucial role in the catalytic oxidation of linalool. Therefore, since that the $Na_7PW_{11}O_{39}$-catalyzed reaction achieved a total conversion with a 2 : 1 ratio of H_2O_2 to linalool, we investigate what was the

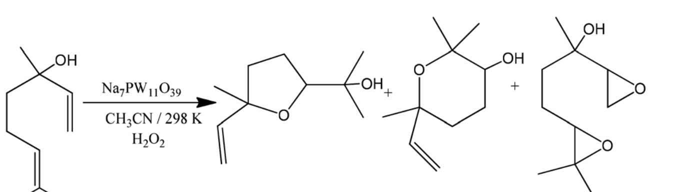

(1) (1a) (1b) (1c)

Scheme 1 Linalool oxidation by H_2O_2 in presence of $Na_7PW_{11}O_{39}$ catalyst.

Open Access Article. Published on 21 February 2020. Downloaded on 12/9/2025 2:17:52 PM.
This article is licensed under a Creative Commons Attribution-NonCommercial 3.0 Unported Licence.

effect on conversion and selectivity using a lower load of oxidant (*ca.* 1 : 1.5 and 1 : 1, Fig. SM9†).

As shown in Fig. SM9a,† the conversion of linalool to linalool oxides and diepoxide increased gradually with the increase of the amount of oxidant. The final conversions after 4 h of reaction were *ca.* 38%, 74% and 100%, when the proportions of H_2O_2 to linalool were 1 : 1, 1 : 1.5 and 1 : 2 respectively. Nonetheless, the final selectivity was approximately the same; 66%, 27% and 7%, for (**1a**), (**1b**) and (**1c**) products, respectively (Fig. SM9b†). When the reactions were carried out in the absence of the catalyst, no oxidation product was detected, regardless of the oxidant load.

3.2.3. Insights on the mechanism for linalool oxides synthesis. We suppose that the excess of peroxide is needed to peroxidize the lacunar sodium phosphotungstate catalyst as depicted in Scheme 2. Literature has reported the same phenomena for reactions of oxidation with H_2O_2 in the presence of tungsten catalysts (Scheme SM2†).[1,2,36]

Thus, it is plausible that the intermediate **1** may be formed, which may transfer the oxygen atom to the double bond of the linalool. This transformation primarily results in an epoxide, which may be easily cyclized to give the corresponding ether derivatives (*i.e.*, linalool oxides; **1a** and **1b**) bearing an additional hydroxyl group. Therefore, we believe that the formation of epoxide is essential for that the reaction continuance (Scheme 2). In Scheme 2, we will demonstrate how the epoxide is converted to product (**1a**) or (**1b**).

The intramolecular nucleophilic attack of the hydroxyl group belonging to linalool epoxide is the key-step that governs the reaction selectivity. After the formation of epoxide, its oxirane ring maybe then opened when the electron pairs of hydroxyl group attack the less hindered electrophilic carbon. This intramolecular cyclization step results in the tetrahydrofuran, after a proton transfer to the anionic intermediate (route a, Scheme 2).

Conversely, when the pair of electrons of the hydroxyl group attack the more hindered electrophilic carbon, the tetrahydropyran is the product obtained (route b, Scheme 2). Note that with the epoxides, the regioselectivity is not as simple, even with acid catalysts, the A_ND_N substitution at a primary carbon atom is very fast.[35,36]

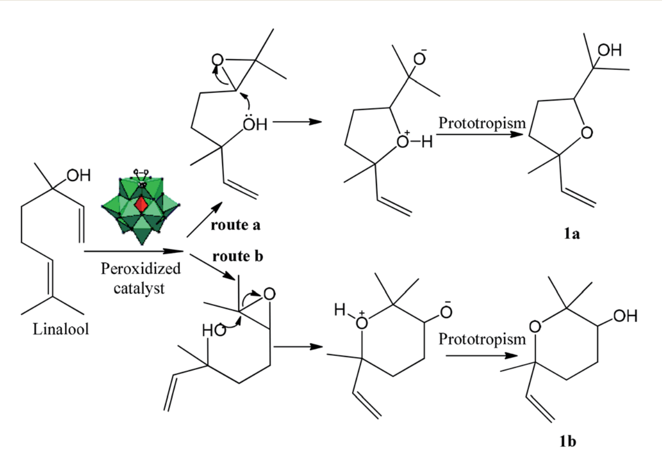

Scheme 2 Possible reaction pathway for the formation of (1a) and (1b) linalool oxides.

3.2.4. Effect of catalyst load. The catalyst load is another essential feature that may affect either conversion or reaction selectivity. Herein, we have assessed this effect in concentration range of 0.083 to 0.5 mol% (Fig. 7).

When we investigated the effect of H_2O_2 load, we have found that while the reaction conversions were strongly affected, the reaction selectivity remained almost unaltered. The variation of the catalyst load triggered the same effect. The reaction selectivity was practically constant, regardless of the catalyst load; conversely, an increase of the catalyst concentration of 0.083 to 0.33 mol%, raised the conversions of 59 to 100%.

3.2.5. Effects of temperature on the $Na_7PW_{11}O_{39}$-catalyzed oxidation of linalool by H_2O_2. To assess this effect, it was required that the $Na_7PW_{11}O_{39}$ catalyst had a concentration lower than that employed in the majority of the other reactions (*ca.* < 0.33 mol%), since that at room temperature, the conversion achieved practically 100% after 1 h of reaction. Therefore, we selected the lowest catalyst concentration used in Fig. 7 (*ca.* 0083 mol%).

Although at the studied concentration the initial rates of the reactions have been close, the exothermic character of the oxidation of linalool was confirmed by the results shown in Fig. 8a. Undoubtedly, it was verified that the linalool oxidation to oxides and diepoxide was more selective at room temperature. Nonetheless, from Fig. 8b we can also conclude that high temperatures increased the diepoxide selectivity and reduced the formation of the tetrahydrofuran derivative.

3.2.6. Effect of terpene substrate on $Na_7PW_{11}O_{39}$-catalyzed oxidation reaction with H_2O_2. We have selected different alcohols; primary (β-citronellol), allylic (geraniol), tertiary (α-terpineol) as substrates (Fig. SM10†). All these alcohols have a double bond which may potentially be epoxidized, resulting in epoxides that may subsequently undergo nucleophilic addition reactions. The kinetics curves are presented in Fig. 9.

When an allylic alcohol (*i.e.*, geraniol, Fig. SM10†) was the substrate, a complete conversion within 4 hours of reaction was achieved with a high selectivity for geraniol-epoxide (*ca.* 89%), meaning that only the allylic double bond of alcohol was reactive, while the more hindered double bond which remained intact.

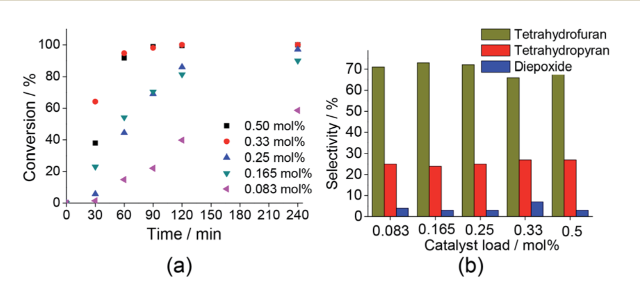

Fig. 7 Impacts of catalyst load on the conversion (a) and products selectivity (b) of $Na_7PW_{11}O_{39}$-catalayzed oxidation reaction of linalool with H_2O_2. [a]Reaction conditions: linalool (2.75 mmol); H_2O_2 (5.5 mmol); temperature (298 K); CH_3CN (10 mL).

Open Access Article. Published on 21 February 2020. Downloaded on 12/9/2025 2:17:52 PM.
This article is licensed under a Creative Commons Attribution-NonCommercial 3.0 Unported Licence.

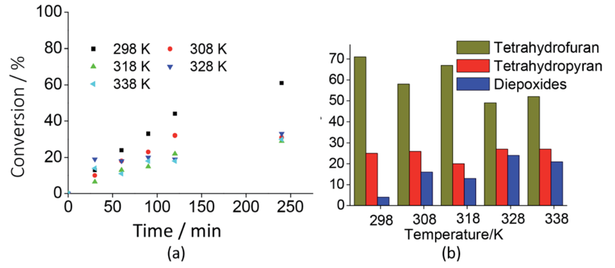

Fig. 8 Effects of temperature on the conversion (a) and selectivity (b) of $Na_7PW_{11}O_{39}$-catalyzed oxidation reactions of linalool with H_2O_2. [a]Reaction conditions: linalool (2.75 mmol); H_2O_2 (5.5 mmol); $Na_7PW_{11}O_{39}$ (0.083 mol%); CH_3CN (10 mL).

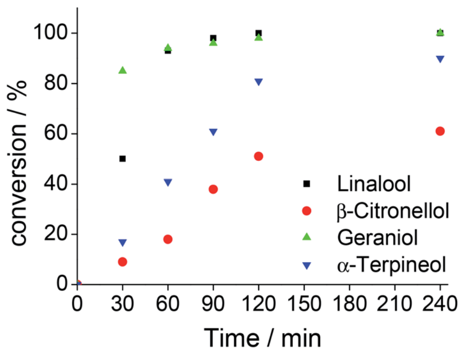

Fig. 9 Oxidation of different terpenic alcohols with hydrogen peroxide in $Na_7PW_{11}O_{39}$-catalyzed reactions. [a]Reaction conditions: alcohol (2.75 mmol); H_2O_2 (5.5 mmol); $Na_7PW_{11}O_{39}$ (0.33 mol%); temperature (298 K); CH_3CN (10 mL).

The primary alcohol (*i.e.*, β-citronellol, Fig. SM10†) was less active than the allylic alcohol; only a conversion of 61% was achieved, with a high epoxide selectivity. Solely traces of aldehydes were detected. The tertiary cyclic alcohol (α-terpineol, Fig. SM10†) was very reactive; a conversion close of *ca.* 90% was achieved with a selectivity of 39, 34 and 27% for keto-alcohol, epoxide and glycol, respectively. We suppose that the glycol was formed through the initial epoxidation of the double bond and subsequent opening of the oxirane ring of epoxide, triggered by nucleophilic attack water present in the oxidant.

4. Conclusions

In this work, we developed an efficient synthesis route of the linalool oxides using an environmentally benign oxidant (*i.e.*, H_2O_2) in lacunar $Na_7PW_{11}O_{39}$-catalyzed reactions at room temperature. Three valuable compounds were selectively obtained after an adequate adjust of reaction parameters; the 2-(5-methyl-5-vinyltetrahydrofuran-2-yl propan-2-ol) (*cis*/*trans* 1 : 1 proportion, **1a**) and 2,2,6-trimethyl-6-vinyltetrahydro-2*H*-pyran-3-ol (*cis*/*trans* 1 : 1 proportion, **1b**) products were the oxides obtained. A diepoxide product (**1c**) was also formed. The excellent performance of the catalyst was assigned to the removal of one WO unit on the saturated anion (*i.e.*, $PW_{12}O_{40}{}^{7-}$), to form the catalytic active lacunar sodium Keggin phosphotungstate ($Na_7PW_{11}O_{39}$). The maximum selectivity combined toward the main products was close to 100%, with a conversion virtually complete of the linalool. The process described herein has attractive aspects; the reactions were performed at room temperature, the catalyst was easily synthesized and achieved excellent catalytic performance, being also efficiently recovered and reused. Therefore, this route demonstrated to be very suitable for the conversion of linalool into linalool oxides, which are important intermediates in chiral synthesis. In addition, $Na_7PW_{11}O_{39}$ catalyst efficiently converted the geraniol, β-citronellol and α-terpineol to their oxidation products (mainly epoxides) at room temperature.

Conflicts of interest

There are no conflicts to declare.

Acknowledgements

The authors are grateful for the financial support from CNPq and FAPEMIG (Brasil). This study was financed in part by the Coordenação de Aperfeiçoamento de Pessoal de Nível Superior – Brasil (CAPES) – Finance Code 001.

References

1 M. J. da Silva, P. H. S. Andrade, S. O. Ferreira, C. B. Vilanculo and C. M. Oliveira, *Catal. Lett.*, 2018, **148**, 2516.
2 L. A. S. Viana, G. R. N. da Silva and M. J. da Silva, *Catal. Lett.*, 2018, **148**, 374.
3 S. Serra and D. De Simeis, *Catalysts*, 2018, **8**, 362.
4 T. L. B Boivin, *Tetrahedron*, 1987, **43**, 3309.
5 B. Azaad and S. Lakshmipathi, *Atmos. Environ.*, 2018, **189**, 235.
6 E. M. Elgendy and M. Y. Semeih, *Arabian J. Chem.*, 2019, **12**, 966.
7 M. G. Kim, S. M. Kim, J. H. Min, O. K. Kwon, M. H. Park, J. W. Park, H. I. Ahn, J. Y. Hwang, S. R. Oh, J. W. Lee and K. S. Ahn, *Int. Immunopharmacol.*, 2019, **74**, 105706.
8 K. C. Nicolaou, C. V. C. Prasad, P. K. Somers and C. K. Hwang, *J. Am. Chem. Soc.*, 1989, **111**, 5330.
9 N. M. Nasir, K. Ermanis and P. A. Clarke, *Org. Biomol. Chem.*, 2014, **12**, 3323.
10 S. S. Wang and G. Y. Yang, *Chem. Rev.*, 2015, **115**(11), 4893.
11 Z. Guo, B. Liu, Q. Zhang, W. Deng and Y. Yang, *Chem. Soc. Rev.*, 2014, **43**(10), 3480.
12 P. T. Anastas and M. M. Kirchhoff, *Acc. Chem. Res.*, 2002, **35**(9), 686.
13 M. J. da Silva, L. C. de Andrade Leles, S. O. Ferreira, R. C. da Silva, K. de V. Viveiros, D. M. Chaves and P. F. Pinheiro, *Chem. Select*, 2019, **4**, 7665.
14 I. V. Kozhevnikov, *J. Mol. Catal. A: Chem.*, 2007, **262**(1–2), 86.
15 M. J. da Silva, P. H. S. Andrade, S. O. Ferreira, C. B. Vilanculo and C. M. Oliveira, *Catal. Lett.*, 2018, **148**, 2516.
16 F. Cavani, *Catal. Today*, 1998, **41**(1–3), 73.
17 M. J. da Silva, *Curr. Org. Chem.*, 2016, **20**, 1.

 This journal is © The Royal Society of Chemistry 2020

18 A. L. P. Meireles, K. A. S. Rocha, I. V. Kozhevnikov and E. V. Gusevskaya, *Appl. Catal., A*, 2011, **82**, 409.
19 R. Karcz, P. Niemiec, K. Pamin, J. Połtowicz, J. Kryściak-Czerwenka, B. D. Napruszewska, A. Michalik-Zym, M. Witko, R. Tokarz-Sobieraj and E. M. Serwicka, *Appl. Catal., A*, 2017, **542**, 317.
20 M. J. da Silva and C. M. de Oliveira, *Curr. Catal.*, 2018, **7**, 26.
21 L. Li, B. Liu, Z. Wu, X. Yuan and H. Luo, *Chem. Eng. J.*, 2015, **280**, 670.
22 K. Kamata, M. Kotani, K. Yamaguchi, S. Hikichi and N. Mizuno, *Chem.–Eur. J.*, 2007, **13**, 639.
23 N. C. Coronel and M. J. da Silva, *J. Cluster Sci.*, 2018, **29**, 195.
24 M. J. da Silva, L. C. de Andrade Leles, R. Natalino, S. O. Ferreira and N. C. Coronel, *Catal. Lett.*, 2018, **148**, 1202.
25 S. Rana and K. M. Parida, *Catal. Sci. Technol.*, 2012, **2**, 979.
26 R. Tayebee, *Asian J. Chem.*, 2008, **20**, 8.
27 L. R. Pizzio, P. G. Vásquez, C. V. Cáceres and M. N. Blanco, *Appl. Catal., A*, 2003, **256**, 125.
28 J. B. Moffat, *Metal-Oxygen Clusters: The Surface and Catalytic Properties of Heteropoly Oxometalates*, Plenum, New York, 2001.
29 G. P. Romanelli, J. C. Autino, M. N. Blanco and L. R. Pizzio, *Appl. Catal., A*, 2005, **295**, 209.
30 L. R. Pizzio and M. R. Blanco, *Microporous Mesoporous Mater.*, 2007, **103**, 40.
31 D. Bajuk-Bogdanovi, I. Holclajtner-Antunonovi, M. Todorovi, U. B. Mio and J. Zakakrzewska, *J. Serb. Chem. Soc.*, 2008, **73**, 197.
32 J. H. Choi, J. K. Kim, D. R. Park, T. H. Kang, J. H. Song and I. K. Song, *J. Mol. Catal. A: Chem.*, 2013, **371**, 111.
33 S. Das and T. Punniyamurthy, *Tetrahedron Lett.*, 2003, **44**, 6033.
34 J. Clayden, N. Greeves, S. Warren and P. Wothers. *Organic Chemistry*. Oxford, 2000.
35 T. M. khomenko, L. E. Tatarova, D. V. Korchagina and V. A. Barkhash, *Russ. J. Org. Chem.*, 2002, **38**, 498.
36 C. B. Vilanculo, M. J. da Silva, S. O. Ferreira and M. G. Teixeira, *Mol. Catal.*, 2019, **478**, 110589.

Open Access Article. Published on 21 February 2020. Downloaded on 12/9/2025 2:17:52 PM.
This article is licensed under a Creative Commons Attribution-NonCommercial 3.0 Unported Licence.